Graduate Training Center of Neuroscience

Computational Neuroscience

Investigating the Cell Type Heterogeneity of *Drosophila melanogaster* T4 Motion-Detection Neurons Using a Connectome-Constrained Model

Laboratory report

presented by

Byoungsoo Kim

The study was supervised by

Zinovia Stefanidi

Prof. Dr. Jakob H. Macke

Machine Learning in Science, Eberhard Karls Universität Tübingen, Tübingen, Germany.

Dr. Srinivas C. Turaga

Janelia Research Campus, Howard Hughes Medical Institute, Ashburn, VA, USA.

Duration of lab rotation: 2025.01.07 - 2025.03.09

Date of submission: 2025.03.28

Abstract

Motion detection is a universal feature of most animals' visual systems, and *Drosophila melanogaster*'s mechanism is notably well-studied. Previous reports [1] [2] highlight heterogeneity in T4 cell tuning directions, though the precise number of subtypes remains debated. Here, I investigated the directional tuning properties of the fly's T4 motion-detection neurons using a connectome-constrained model. Building on the recently published connectome dataset [3] I employed three different approaches: analyzing the raw connectivity graph, simulating an untrained connectome-constrained network, and simulating trained connectome-constrained networks. All methods indicate that T4 neurons cluster around four distinct directions—roughly, but not strictly, cardinal. Additionally, T4 cells in layers C and D of the lobula plate exhibit broader directional responsiveness compared to those in layers A and B. While these findings align more closely with earlier work [1], further investigation—such as incorporating the 3D structure of the fly's eye and examining the impact of model initialization—remains necessary.

Acknowledgements

I am sincerely grateful to Professor Jakob H. Macke and all members of the Machine Learning in Science group at the University of Tübingen for the opportunity to work on this project. I extend special thanks to Zinovia Stefanidi for her close supervision and unwavering support. I also greatly appreciate the invaluable guidance from Professor Macke and Dr. Srinivas C. Turaga, as well as the active discussions and guidance provided by every member of the Flyvision team.

Contents

Chapter 1

Introduction

Imagine gazing at a clear summer sky when a bird suddenly enters your view—you instantly notice its presence and the direction from which it comes: it's a falcon. Detecting movement on the ground, the falcon locks onto a mouse and descends. Noticing the slightest motion, the mouse senses danger and darts away. Motion detection is a universal feature of visual pathways in many animals, and the visual system of *Drosophila melanogaster* contains one of the most widely studied motion detection mechanisms.

To understand the fly's motion detection mechanisms, one can begin by examining its compound eye structure. The fly's eye comprises approximately 800 ommatidia, arranged in a hexagonal lattice[5]. This same hexagonal lattice is maintained throughout the deeper layers of the optic lobe. Notably, similar cell types are present in each column of this three-dimensional lattice, and the connections between these cells are highly stereotyped[4]. Among these cell types, T4 and T5 cells are primarily responsible for motion detection. They achieve their function through nonlinear interactions among the input cells' signals and their spatial organization[6]. For the scope of this project, I will focus on the T4 cells.

T4 cells receive input from multiple sources, with five major inputs coming from the Mi9, Tm3, Mi1, Mi4, and C3 cell types[6]. Mi9 and the combined Mi4+C3 inputs provide a delayed inhibitory signal to T4 cells, whereas the Tm3+Mi1 inputs supply a fast excitatory signal. The spatial arrangement of these inputs determines the tuning direction of the T4 cells. For example, if inputs from Mi9 neurons originate in the left column, those from Tm3+Mi1 neurons in the central column, and those from Mi4+C3 neurons in the right column, then that T4 cell becomes selective for rightward motion.

One might ask how many directions T4 cells are selective for. In the pioneering study by Maisak et al.[1], which demonstrated the motion detection properties of T4 cells, the authors reported that these cells are tuned to four cardinal directions. At the lobula plate—where the axon terminals of T4 cells project—each direction-tuned population is anatomically distinct, residing in one of four sublayers. Specifically, layer A houses T4 cells tuned to rightward motion (0°), layer B to leftward motion (180°), layer C to upward motion (90°), and layer D to downward motion (270°).

However, in the recent report from Henning et al.[2], it is argued that T4 cells continuously map circular directions, and at the population level, the cells are tuned to six different diagonal directions, matching the degrees of freedom of the fly's global motion patterns. In detail, the T4 neurons at layer A of the lobula plate are tuned to 30° and 330° rather than 0°, and the neurons at layer B to 150° and 210° rather than 180°. Moreover, the paper reported that the T4 cells at layers A and B are tuned to a wider range of directions than those at layers C and D.

Based on these previous reports, we became curious about whether the directional tuning properties of T4 cells could be predicted from their connectivity graph with other cells in the optic lobe. Most interestingly, since the spatial arrangement of the input cells plays a crucial role in the tuning directions of T4 neurons, one might expect to observe traces of this relationship in their raw connectivity patterns. The very recently published connectome dataset from Nern et al.[3] fully reconstructed the fly's right optic lobe. Although the connections between cell types within each column of the optic lobe are stereotypical, this connectome provides an opportunity to examine the heterogeneity of connections between different columns, which might give rise to varying directional tuning properties of T4 neurons.

One approach to predicting a cell's function from its neuronal wiring diagram is to analyze the raw connectivity graph. Seung demonstrated this approach in his recent paper[7] by predicting the function of Dm3 and TmY cells as they encode the angular direction of a local visual feature. Here, he used only the raw connectivity graph to predict the receptive fields of those cells.

Another interesting approach is to simulate neural activity by constructing a neural network that mirrors the connectome's connectivity. In Shiu et al.[8], the authors built a whole-brain computational model of the fly using a

leaky integrate-and-fire neuronal model, adapting the connectivity graph from the FlyWire dataset [9]. They claimed that this approach can predict how sensory inputs are transformed into motor behaviors.

Lastly, previous work from our lab [4] demonstrated that training connectome-constrained networks with deep learning methods can accurately predict the known activity of neurons within the fly's optic lobe. In particular, this approach correctly predicted the ON- and OFF-motion selectivity of T4 and T5 cells. However, in that study, the authors assumed the translational invariance of cell types and their connections across different columns of the hexagonal lattice.

In this project, I combined three approaches to predict the motion tuning properties of T4 cells using the recently published fly's optic lobe connectome dataset [3]. First, I predicted their tuning directions directly from the raw connectivity graph. Second, I simulated the fly's optic lobe connectome-constrained network to estimate the tuning properties of T4 neurons. Lastly, by training the same connectome-constrained network, I predicted the tuning properties of the cells. The results suggested that, at the population level, T4 cells are tuned to 4 distinct, but not cardinal, directions rather than 6 different diagonal directions.

Chapter 2

Results

2.1 Prediction of T4 cell tuning directions based on the raw connectivity graph

To predict the tuning directions of all T4 cells, I considered monosynaptic inputs from the three major cell types. Since the spatial arrangement of these inputs is critical for motion detection, I traced their relative positions with respect to the target T4 cells and computed the predicted tuning directions for each cell (see Methods).

Based on predictions from the raw connectivity graph, T4 cells were predominantly tuned to four distinct directions—approximately 0°, 180°, 90°, and 270° for layers A, B, C, and D, respectively (Fig.1). Moreover, at every layer, neurons exhibited a broad distribution of tuning directions spanning more than 90° (Fig.1a), indicating that T4 cells collectively map the full range of directions.

These results align with the findings of Maisak et al.[1], although the cells in our study were not strictly tuned to the four cardinal directions. Notably, cells in layers C and D exhibited tuning centered at angles significantly shifted from the cardinal directions (Fig.1b). In contrast to Henning et al.[2], not only are the cells in layers A and B tuned to a single predominant direction (see the first two columns of Fig.1), but T4 neurons in layers C and D are also tuned to a broader range of angles than those in layers A and B (Fig.1b).

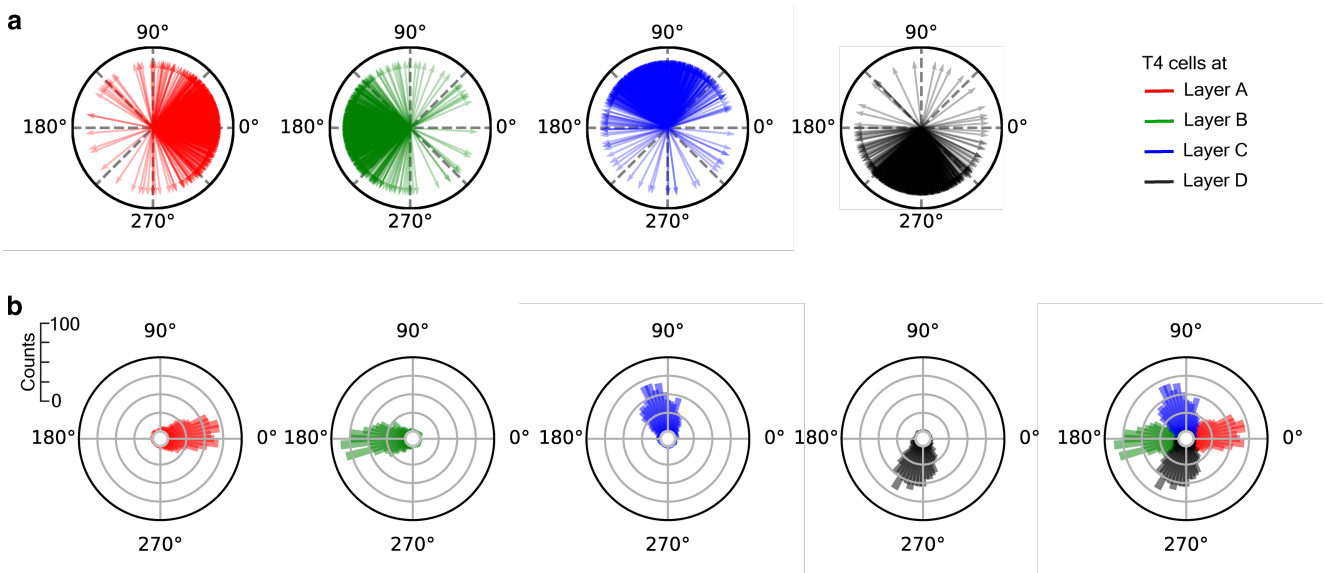

Figure 1. Prediction of T4 cell tuning directions from the neuronal wiring diagram

a, T4 tuning direction vectors; the angular position of each vector represents the tuning direction of a T4 cell, while the vector length is arbitrary. **b**, Circular histogram of T4 tuning directions; the panel on the right displays all T4 cells.

2.2 Prediction of T4 cell tuning directions using an untrained, connectome-constrained model

Next, I simulated neural activity across the entire optic lobe connectome network to predict T4 cells' tuning directions. After constructing a connectome-constrained network and initializing each neuron's parameters, I presented visual

stimuli (Fig.2a). Moving ON-edges in 12 different directions (at 30° intervals starting from 0°) were used to obtain activity traces from all T4 cells (see Methods).

To characterize the tuning properties of a given T4 cell, I used two measurements: the preferred direction (PD) and the direction selectivity index (DSI), computed from the cell's activity traces in response to different stimulus directions (Fig.2b). PD indicates the direction to which a T4 neuron is most responsive, while DSI quantifies the specificity of this tuning (see Methods).

From the prediction with simulating an untrained network, T4 cells primarily exhibited tuning in four different directions, while neurons in layers C and D responded over a wider range of angles than those in layers A and B (Fig.2c,d)—matching the result from investigating the raw connectivity graph.

Notably, the dynamic range of responses is narrow (Fig.2b), resulting in small DSI values (Fig.2c). This tendency is expected because, in an untrained network, a given stimulus may dissipate as it propagates through deeper layers. Consequently, many T4 neurons exhibit effectively 0 DSI. Nevertheless, this analysis demonstrates that the fly's optic lobe network is inherently wired to be sensitive to different motion directions. Moreover, the tuning directions at each layer remain distinguishable (Fig.2d).

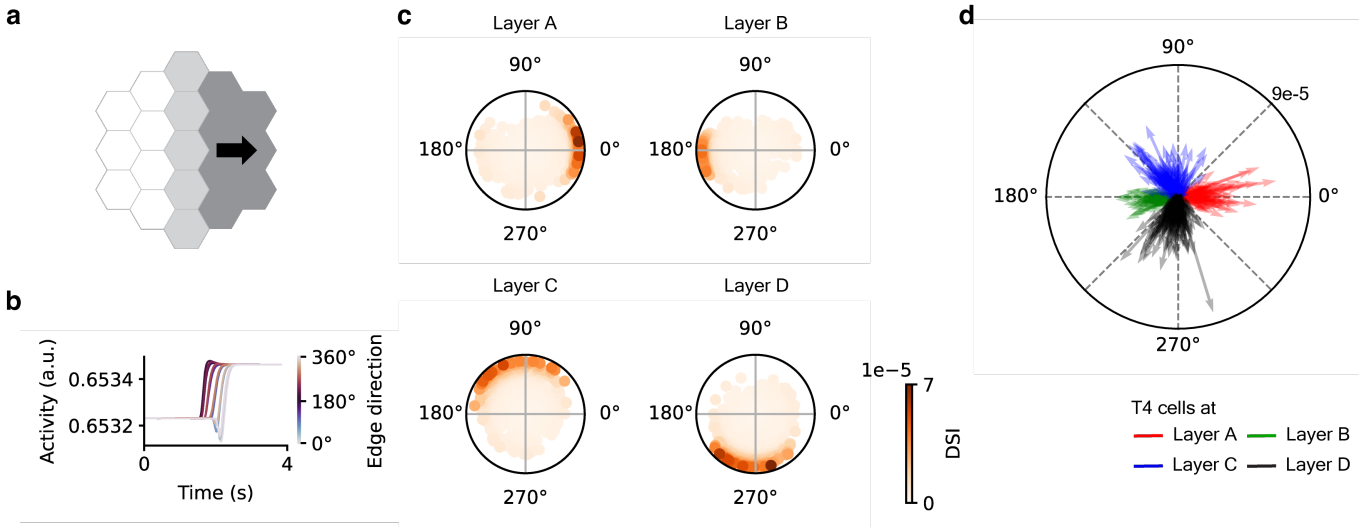

Figure 2. Prediction of T4 cell tuning directions from an untrained network

a, Schematic of a stimulus; an ON-edge moving toward the 0° direction. 12 different directions were presented. **b**, Example responses of a T4 cell to all 12 ON-edge directions. **c**, Tuning properties of T4 neurons at each layer; each dot represents a cell, with its angular position corresponding to the PD and its color and radial distance reflecting the DSI. **d**, T4 tuning direction vectors; the angular position of each vector indicates a cell's PD, while its length corresponds to the DSI.

2.3 Prediction of T4 cell tuning directions using a trained, connectome-constrained model

Lastly, I investigated a trained connectome-constrained model of the fly's optic lobe to predict T4 neurons' tuning directions. The same connectome-constrained network was used for training, but with a different neuronal model (see Methods). To compute the tuning properties from the trained model, I followed the same simulation procedure as for the untrained network, analyzing the neuronal activities obtained from simulating the trained network (Fig.3a).

Prediction from a trained connectome-constrained model aligns with the two previous findings—T4 cells are tuned to four distinct directions (Fig.3b,c). However, the tendency for cells at layers C and D to exhibit collectively wider tuning angles than those at layers A and B is not significant. Moreover, cells at each layer are tuned to a narrower range of angles, resulting in a range of directions that are poorly represented between the four distinct directions. In addition, while the cells were not strictly tuned to cardinal directions, their tuning clustered more closely around these directions, particularly at layers C and D (Fig.3c).

In comparison to the result from simulating an untrained network, a few distinctions emerged. First, the activity traces display a wider dynamic range, leading to DSI values ranging from 0 to 1 (Fig.3b), which is consistent with previous work from our group[4]. Second, the PDs are now tuned to a narrower range of angles across all layers, while still aligning with the expected directions at each layer (Fig.3c).

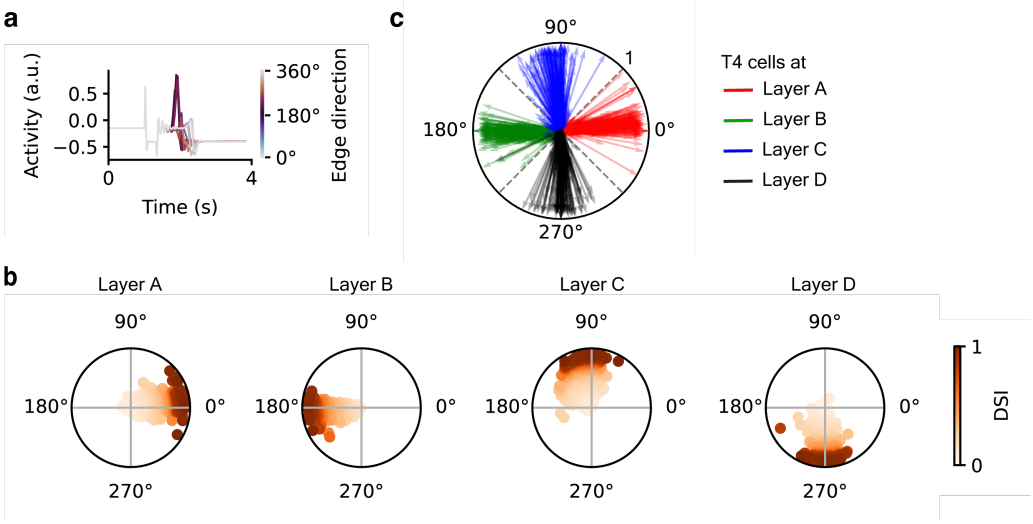

Figure 3. Prediction of T4 cell tuning directions from a trained network

a, Example responses of a T4 cell to all 12 ON-edge directions. **b**, Tuning properties of T4 neurons at each layer; each dot represents a cell, with its angular position corresponding to the PD and its color and radial distance reflecting the DSI. **c**, T4 tuning direction vectors; the angular position of each vector indicates a cell's PD, while its length corresponds to the DSI.

Chapter 3

Discussion

In this study, I predicted the motion direction to which each T4 cell is tuned using three different approaches: predicting with a raw connectivity graph, simulating an untrained, connectome-constrained model, and simulating a trained, connectome-constrained model. The results suggest that T4 neurons are primarily tuned to four different directions, though not strictly to the cardinal directions. Moreover, cells in layers C and D tend to be responsive to a wider range of directions than those in layers A and B. This finding aligns better with the report from Maisak et al.[1] than with that of Henning et al.[2]. However, further investigation is necessary to determine that T4 cells are not tuned to six different diagonal directions.

First, for the simulations in this study, I assumed a flat fly's eye. However, in animal experiments—including those by Maisak et al.[1] and Henning et al.[2]—the fly's eye exhibits a three-dimensional structure. Recently, Zhao et al.[10] claimed that the non-cardinal directional tuning of motion detection cells in *Drosophila melanogaster* originates from a non-uniform sampling of visual space. In other words, due to the curvature of the fly's compound eye, different tuning directions across 360° emerge, even though each T4 cell's dendrite orientation remains consistent within each layer. Therefore, incorporating the 3D structure of the fly's compound eye into the simulation might yield different motion tuning orientations for each T4 cell.

Further investigation into the anatomical positions of T4 cells is another analysis that would be interesting to pursue. In Henning et al.[2], it was reported that the two subtypes within layers A and B can be anatomically differentiated along the dorsoventral axis at the lobula plate. The connectome dataset[3] provides relevant information about the locations of all T4 cells' axons at the lobula plate, making an in-depth comparison possible.

The report that the fly eye's curvature enables tuning directions beyond the cardinal ones[10] also raises the question of whether the input cells to T4s are spatially organized in a way that reflects the eye's three-dimensional structure. I conducted a brief investigation by examining the spatial organization of tuning angles and the distances between input cell types, specifically Mi9 and Mi4+C3 (Extended Fig.1). From this analysis, I did not find any evidence of spatially organized patterns. However, a more thorough investigation—including input cells beyond monosynaptic connections—deserves further study.

In Seung's study[7], he investigated the receptive fields of neurons by considering both monosynaptic and disynaptic inputs, and he predicted that disynaptic inputs are responsible for constructing peripheral receptive fields. A similar analysis could be applied to the motion detection pathways of T4 cells; considering disynaptic inputs might diversify the tuning directions of T4 neurons.

Lastly, the simulation results for both untrained and trained models depend on the initialization. For instance, the tuning properties of another trained network with different initial parameters (Extended Fig.2) were different from those shown earlier (Fig.3b). Lappalainen et al.[4] used an ensemble of models to explore the properties of individual neurons, which can address this issue. Adopting a similar ensemble approach for both simulation types would be crucial for thoroughly investigating the tuning properties of all T4 cells.

Chapter 4

Methods

4.1 Predicting tuning direction from the raw connectivity graph

I predicted the tuning direction of each T4 cell using the locations of the major input cell types within the hexagonal lattice. The three major input cell types considered were Mi9, Mi4, and C3, which I grouped into two categories—Mi9 (group1), and Mi4+C3 (group2)—based on previous literature[6].

For each cell, a unique location in the hexagonal lattice (u, v coordinates) was assigned using a spatial hexagonal coordinate method, ensuring that no two cells of the same type occupied the same position. The ground truth location within the fly's eye was derived from the anatomical positions of cells in the medulla. Let's consider a set of inputs from the defined groups to a T4 cell.

$$\text{u,v coordinates of group1 cells} : \{(u_1^1, v_1^1), ..., ((u_N^1, v_N^1))\} \tag{4.1}$$

$$\text{corresponding input weights} : \{w_1^1, ..., w_N^1)\} \tag{4.2}$$

$$\text{u,v coordinates of group2 cells} : (u_1^2, v_1^2), ...((u_M^2, v_M^2)) \tag{4.3}$$

$$\text{corresponding input weights} : \{w_1^2, ..., w_M^2)\} \tag{4.4}$$

, where input weights were from synapse counts obtained from the connectome dataset[3]. For each group of input cells, weighted average location was calculated as such:

$$(\bar{u}_1^j, \bar{v}_1^j) = (\frac{\Sigma_{i=1}^N w_i^j u_i^j}{N}, \frac{\Sigma_{i=1}^N w_i^j v_i^j}{N}) \tag{4.5}$$
$$j = 1, 2$$

Then the predicted tuning vector was defined as such:

$$(\text{predicted tuning vector}) \equiv (\bar{u}_1^2 - \bar{u}_1^1, \bar{v}_1^2 - \bar{v}_1^1) \tag{4.6}$$

The direction of each vector indicates the tuning direction of a given cell, while its magnitude corresponds to the distance between the input cells. Predicted tuning vectors were computed for all T4 cells.

4.2 Predicting tuning direction from a untrained, connectome-constrained network

4.2.1 Connectome-constrained network model

The connectivity graph was directly adapted from Nern et al.[3]. For the neuronal dynamics and the connections between them, we followed these equations:

(passive point neuron voltage dynamics)

$$\tau_{t_i} \dot{V}_i = -V_i + \Sigma_j s_{ij} + V_{t_i}^{rest} \tag{4.7}$$

(instantaneous graded release synapses)

$$s_{ij} = w_{ij} f(V_j) \tag{4.8}$$

$$w_{ij} = \alpha_{t_i t_j} \sigma_{t_i t_j} N_{ij} \tag{4.9}$$

, where $\alpha_{t_i t_j}$ is a scaling factor, $\sigma_{t_i t_j}$ is a sign of a synapse between cell types t_i and t_j. N_{ij} is a synapse count between two neurons i and j. The function f mimics the nonlinear release of neurotransmitters.

4.2.2 Simulating a connectome-constrained network model

To simulate the network model, we first initialized each parameter according to the following constraints:

$$\alpha_{t_i t_j} = \frac{0.01}{\langle N_{t_i t_j} \rangle}, \tag{4.10}$$

$$V_{t_i}^{rest} \sim \mathcal{N}(0.5, 0.05) \tag{4.11}$$

A moving ON-edge (see Fig.2a for an example) was presented in 12 different directions (from 0° to 330° in 30° intervals) to the fly's retinal neurons (for more detail, see the method section of Lappalainen et al.[4]). Responses of all T4 cells were recorded during the presentation of the stimuli. Then, tuning properties of the T4 neurons were quantified (see following section **Quantification of tuning property**).

4.3 Predicting tuning direction from a trained, connectome-constrained network

4.3.1 Connectome-constrained network model

The connectivity graph was directly adapted from Nern et al.[3]. For the neuronal dynamics and the connections between them, we followed these equations:

(conductance-based voltage dynamics)

$$\tau_{t_i} \dot{V}_i = -V_i + \Sigma_j (E_{\text{exc|inh}} - V_i) g_{ij} + V_{t_i}^{rest} \tag{4.12}$$

$$g_{ij} = \alpha_{ij} N_{ij} f(V_j) \tag{4.13}$$

, where $E_{\text{exc|inh}}$ is a reversal potential of a neuron, and all other parameters follow the previously established definitions.

4.3.2 Training and simulating connectome-constrained network models

For the training, we followed the same procedure as in Lappalainen et al.[4] using an optic flow task. The trainable parameters included τ_{t_i}, $E_{\text{exc|inh}}$, α_{ij} and $V_{t_i}^{rest}$. This training yielded an ensemble of 50 differently initialized and trained networks.

For each network in the ensemble, we conducted the simulation as previously described, but now using the parameters obtained through training. Then, the tuning properties of the T4 neurons were quantified (see following section **Quantification of tuning property**).

4.4 Quantification of tuning property[4]

4.4.1 Preferred direction (PD)

Preferred direction is defined from the vector sum of the peak response vectors for each stimulus.

$$\text{(preferred direction)} = \arctan\left(\frac{(\Sigma_{i=1}^{12}(\mathbf{r_i}))_\mathbf{y}}{(\Sigma_{i=1}^{12}(\mathbf{r_i}))_\mathbf{x}}\right) \tag{4.14}$$

, where r_i denotes the peak response vector for each stimulus direction for a neuron i.

4.4.2 Direction selectivity index (DSI)

Direction selectivity index is computed by following formula for a neuron i:

$$\text{DSI}_i(I) = \frac{1}{|S|} \sum_{S \in \mathcal{S}} \frac{\left| \sum_{\theta \in \Theta} r_i^{\text{peak}}(I, S, \theta)\, e^{i\theta} \right|}{\max_{I \in \mathcal{I}} \left| \sum_{\theta \in \Theta} r_i^{\text{peak}}(I, S, \theta) \right|} \tag{4.15}$$

, where

$$r_i^{\text{peak}}(I, S, \theta) = \max_n V_i[n](I, S, \theta) \tag{4.16}$$

θ is a movement angle, I is intensity, and S is a speed of moving edges.

Appendix A

Extended Figures

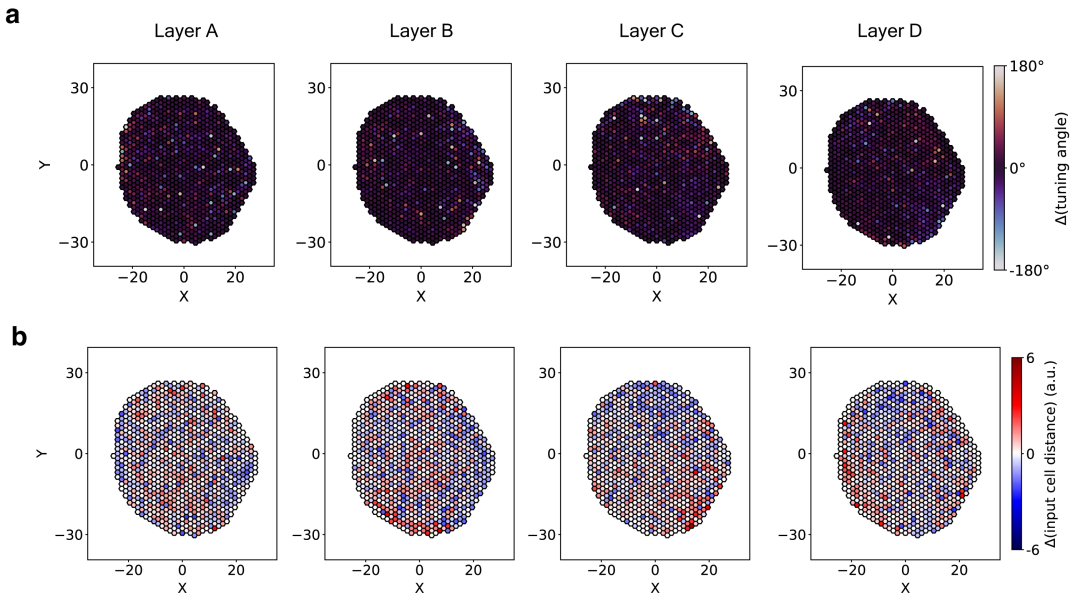

Extended Figure 1. Spatial organization of tuning angles and distance between input cell types to T4 cells

Hexagonal lattice of cells is referenced from the medulla layer. Each hexagon represents a T4 cell. **a**, Spatial organization of relative tuning angles compared to the mean tuning angle at each layer. **b**, Spatial organization of relative distances between Mi9 and Mi4+C3 cell types compared to the mean distance at each layer. The weighted average location for each cell type was computed (see Methods).

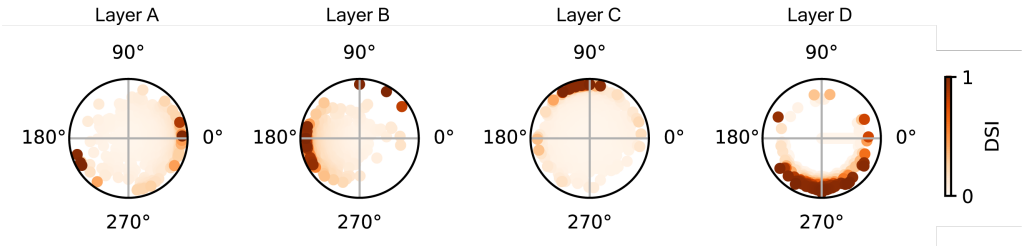

Extended Figure 2. Prediction of T4 cell tuning directions from a trained network with a different initialization

Tuning properties of T4 neurons at each layer; each dot represents a cell, with its angular position corresponding to the PD and its color and radial distance reflecting the DSI.

References

[1] Maisak, M. S. *et al.* A directional tuning map of Drosophila elementary motion detectors. *Nature* **500**, 212–216 (2013). URL https://www.nature.com/articles/nature12320.

[2] Henning, M., Ramos-Traslosheros, G., Gür, B. & Silies, M. Populations of local direction–selective cells encode global motion patterns generated by self-motion. *Science Advances* **8**, eabi7112 (2022). URL https://www.science.org/doi/full/10.1126/sciadv.abi7112.

[3] Nern, A. *et al.* Connectome-driven neural inventory of a complete visual system. *Nature* 1–13 (2025). URL https://www.nature.com/articles/s41586-025-08746-0.

[4] Lappalainen, J. K. *et al.* Connectome-constrained networks predict neural activity across the fly visual system. *Nature* **634**, 1132–1140 (2024). URL https://www.nature.com/articles/s41586-024-07939-3.

[5] Ranganathan, R., Malicki, D. M. & Zuker, C. S. Signal Transduction in Drosophila Photoreceptors. *Annual Review of Neuroscience* **18**, 283–317 (1995). URL https://www.annualreviews.org/content/journals/10.1146/annurev.ne.18.030195.001435.

[6] Borst, A. & Groschner, L. N. How Flies See Motion. *Annual Review of Neuroscience* **46**, 17–37 (2023). URL https://www.annualreviews.org/content/journals/10.1146/annurev-neuro-080422-111929.

[7] Seung, H. S. Predicting visual function by interpreting a neuronal wiring diagram. *Nature* **634**, 113–123 (2024). URL https://www.nature.com/articles/s41586-024-07953-5.

[8] Shiu, P. K. *et al.* A Drosophila computational brain model reveals sensorimotor processing. *Nature* **634**, 210–219 (2024). URL https://www.nature.com/articles/s41586-024-07763-9.

[9] Dorkenwald, S. *et al.* Neuronal wiring diagram of an adult brain. *Nature* **634**, 124–138 (2024). URL https://www.nature.com/articles/s41586-024-07558-y.

[10] Zhao, A. *et al.* Eye structure shapes neuron function in Drosophila motion vision (2022). URL https://www.biorxiv.org/content/10.1101/2022.12.14.520178v1.